

LOW-TEMPERATURE PHASE DIAGRAM OF THE HEAVY-FERMION SUPERCONDUCTOR UPt_3

J.J.M.Franse, K.Bakker, N.H.van Dijk, A.A. Menovsky and A.de Visser

*Van der Waals-Zeeman Laboratorium, Universiteit van Amsterdam Valckenierstraat 65,
1018 XE Amsterdam, The Netherlands*

The transition to the superconducting state of UPt_3 has been studied in specific-heat experiments on polycrystalline and single-crystalline samples in dependence of heat treatment, purity of starting materials and deviations from stoichiometry, as well as on substituted compounds. The concepts behind the splitting of the transition in two anomalies that are 60 mK apart are critically reviewed. The superconducting phase diagram in the B-T plane has been studied with the use of a sensitive dilatometric technique. The three superconducting phases meet at a tetracritical point and all four phase lines are of second order. From the length anomalies at the phase boundaries the pressure derivatives of the phase lines have been determined and the most stable phase under uniaxial pressure along the c-axis has been identified.

1. INTRODUCTION

The superconducting phase diagram in the B-T plane of the heavy-fermion superconductor UPt_3 has been studied during the past few years in detail on pure¹⁻⁶ as well as on substituted⁷ compounds. The main features of this phase diagram are now well established: a multicomponent phase diagram with three different phases that meet at a tetracritical point. The phase diagram of UPt_3 has recently been investigated by means of a parallel-plate capacitance technique in magnetostriction and thermal-expansion measurements for various field and strain directions with respect to the crystallographic directions. From thermodynamic considerations, the behaviour of the different phases under uniaxial pressure has been deduced and the more stable phase under uniaxial pressure along the c-axis has been identified.⁸ The multicomponent phase diagram of UPt_3 is frequently discussed in terms of a symmetry-breaking field that causes a splitting in the transition to the superconducting state⁹⁻¹¹. A candidate for this symmetry-breaking field is the weak-moment (of the order of $0.01 \mu_B$) antiferromagnetic order below 5 K observed in neutron experiments.¹² Substitution studies result in all cases in a fast depression of superconductivity with, in case of Pd substitutions, an appreciable increase

of the distance in temperature between the two superconducting transitions.⁷ On the other hand, at further increasing the Pd concentration to two percent or more, superconductivity is lost and long-range antiferromagnetic order is found with magnetic moments of $0.5 \mu_B$ per formula unit.¹³ These observations suggest a relation between the intensity of the splitting and the magnetic-moment formation in the Pd-substituted alloys and are in line with the existence of a critical uniaxial pressure along the c-axis above which the splitting and the weak moment disappear. A direct link between the splitting of the superconducting transition and the weak-moment antiferromagnetic order, however, remains to be confirmed since for other substitutions (Th and Au) that drive the system towards long-range antiferromagnetic order, no clear effects on the splitting have been reported. Other explanations for the double superconducting transition are looked for as well. For instance, the scenario of two nearly degenerate representations that split the superconducting phase transition in the presence of spontaneous lattice deformations or stacking faults.¹⁴ In this context, we mention the effects of sample purity and atomic defect structure on the superconducting phase diagram of UPt_3 as studied on UPt_{3+x} samples with x-values between -0.06 and 0.06 (nominal values).¹⁵ Although the sharpness of the relevant features are certainly affected by the exact composition, the transition temperature itself and the splitting between the two transitions do not change noticeably. Both series of experiments (alloying and varying the stoichiometry) do not univocally support the concept of either the symmetry-breaking field or the spontaneous lattice deformation c.q. stacking faults behind the double superconducting transition in UPt_3 . In the present contribution we review our studies of the annealing procedures, the purity of starting elements and the deviations from stoichiometry and their effect on the transition to the superconducting state as measured in specific-heat measurements. In addition we report on the phase diagram in the B-T plane as studied in dilatometry experiments.

2. SAMPLE-PREPARATION CONDITIONS AND THERMODYNAMIC PROPERTIES

Specific-heat experiments have been performed on a series of monocrystalline and polycrystalline UPt_3 samples with and without the application of a specific annealing procedure in order to reduce strains or to improve the homogeneity. Some of the results are shown in figure 1 of reference 3. Additionally, monocrystalline samples have been prepared with the addition of boron, applying the same annealing conditions. Boron addition turns out to reduce the value of the residual resistivity and to shift the superconducting transition towards higher temperatures. Three kinds of effect have to be expected from these boron additions: boron reduces the oxygen content of the sample by the formation of B_2O_3 that is deposited at the surface of the melt; interstitial boron atoms expand the lattice; the electronic structure changes by the interstitial atoms. The lowering of the residual resistivity and the shift of T_c towards higher temperatures can be understood in terms of this purification effect and the negative chemical pressure, respectively. In the polycrystalline samples shown in figure 1 of reference 3, the double superconducting transition is hardly visible in contrast to the monocrystalline sample. This is not a general rule since in subsequent studies, the double transition is visible in the specific

heat of polycrystalline samples as well. Our original interpretation of the broad transition in polycrystalline samples, even after the application of an appropriate annealing procedure, was phrased in terms of a distribution of strains caused by the largely anisotropic contraction at cooling UPt_3 from room temperature down to liquid helium temperatures. Uniaxial stress along the hexagonal axis has been shown to reduce the splitting of the superconducting transition temperature¹⁶ and a distribution of stresses will cause a distribution of splittings for the different grains of the polycrystalline material. Depending on the grain size and the presence of preferential orientations, the double transition will be visible in multigrain samples or not. In later studies, the role of lattice defects and lattice anomalies have been emphasized^{17,18} also in relation to the weak magnetic order and the occurrence of a double superconducting transition in this material. Here, we refer to our resistivity and specific-heat studies on non-stoichiometric samples of UPt_3 . The specific heat data for the UPt_{3+x} samples are shown in fig. 1.

The samples have been investigated in X-ray and microprobe experiments with the following conclusions. The non-stoichiometric samples contain small amounts of second phases which is for the $x=0.06$ sample the neighbouring compound UPt_5 and for the $x=0.06$ sample the compound UPt_2 . Both neighbouring compounds do not show superconductivity neither magnetic order. The actual deviation from stoichiometry of the $x = \pm 0.06$ samples is considerably smaller than the nominal composition and is of the order of $x = \pm 0.02$. X-ray photographs show additional lines for the Pt-rich samples which are already observable for the $x=0.03$ sample in agreement with the above conclusion regarding the actual deviation from stoichiometry. The additional lines do not belong to the impurity phases and might point to superstructure lines. Anyhow, there is little effect of the deviations from stoichiometry on the start of the superconductivity and on the temperature splitting of the two superconducting transitions. The splitting is most sharply visible in the U-rich compounds which might be related to a reduced oxygen content by the formation of uranium-oxyde as an impurity phase that does not affect the superconducting properties. In further experiments we investigated the effect of the purity of the starting material on the superconducting properties. Three polycrystalline batches have been produced under identical circumstances with three different qualities of uranium metal. For the uranium metal of the batches #1 and #2, the resistance ratio between room temperature and 4.2 K amounts to 11, whereas for the third batch, batch #3, this ratio is 35, indicating a superior purity of the uranium metal used in preparing batch #3. The specific-heat transition for this latter batch is at the highest temperature and the double feature is most pronounced in this sample, see fig.2. Nevertheless, the batches #1 and #2 show the two-step process clearly as well and no firm conclusion can be drawn from these experiments. Finally, we investigated the effect of the annealing procedure on the superconductive transition for two different batches of single-crystalline samples prepared from the polycrystalline batches #2 and #3. The samples were measured before and after annealing during one week at 950 °C in a standard quartz ampoule or in an ampoule with a special treatment to reduce the oxygen delivery by the quartz ampoule during annealing. Annealing in a reduced oxygen atmosphere certainly improves the superconducting properties as is clear from the data shown in figs 3 and 4. The relevance of an appropriate annealing procedure has recently been stressed by Brison et al.,²⁰ who

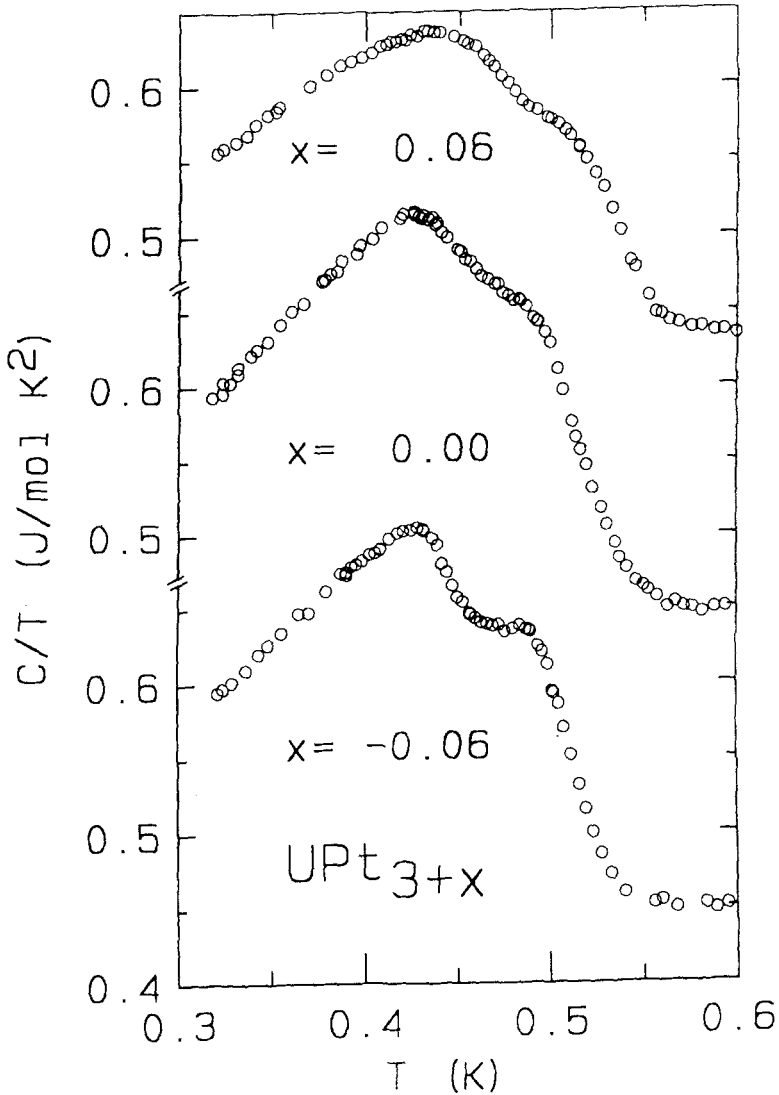


Fig. 1. Specific heat plotted as c/T versus T for UPt_{3+x} samples prepared from a non-stoichiometric melt with nominal x -values of -0.06, 0.00 and 0.06; the samples have been annealed during one week at 950 °C; data from ref.15.

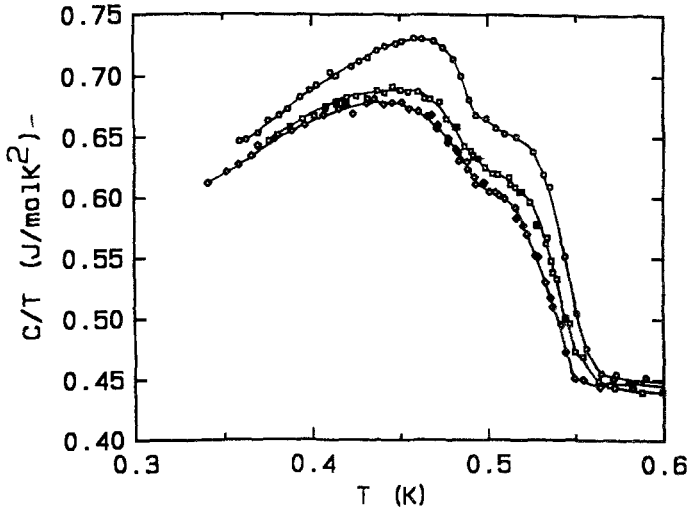


Fig. 2. Specific heat plotted as c/T versus T for three annealed polycrystalline batches of UPt_3 , prepared with uranium metal from different sources; batch #3 with the highest RRR value is indicated by (o); the solid lines are guides to the eye; data from ref.19.

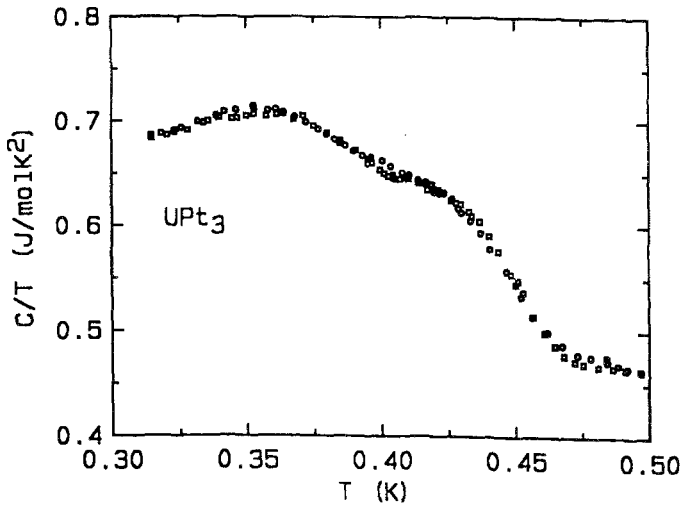


Fig. 3. Specific heat plotted as c/T versus T for single-crystalline UPt_3 before (\square) and after (\circ) annealing at 950°C during one week in a standard quartz ampoule; the starting material was the same as for batch #2 in fig.3; dat from ref.19.

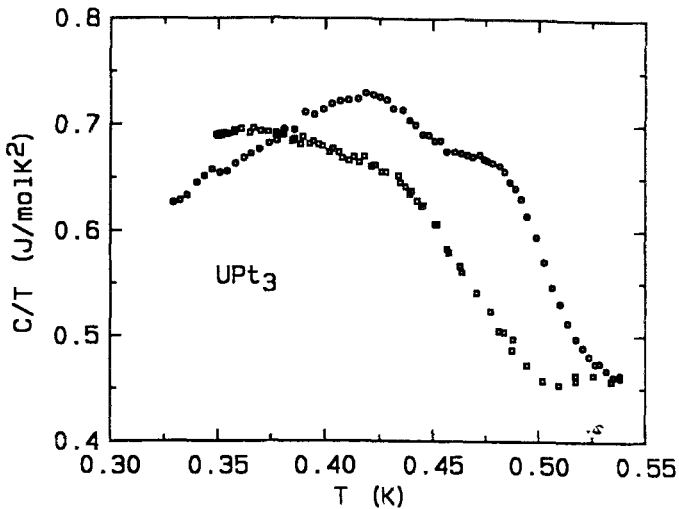


Fig. 4. Specific heat plotted as c/T versus T for single-crystalline UPt_3 before (\square) and after (\circ) annealing at 950°C during one week in a specially prepared quartz ampoule in order to reduce the oxygen delivery by the ampoule at annealing; the starting material was the same as for batch #3 in fig.3; data from ref.19.

showed the importance of the annealing temperature on the low-temperature superconducting properties. The best results were obtained for annealing temperatures between 1200 and 1400°C . Summarising these studies of the double transition to the superconducting state of UPt_3 we conclude, especially on the basis of the experiments on non-stoichiometric UPt_{3+x} compounds, that there is no hard proof for a direct relation between the double transition and lattice imperfections or superstructures, although it is clear from ref. 18 that the double transition is sharpest in samples in which the structural modulations are best developed.

3. IMPURITY STUDIES OF THE SUPERCONDUCTING TRANSITION

The superconducting properties of substituted UPt_3 compounds have been studied in resistivity and specific-heat experiments for U-substitutions by Th and Y and for Pt-substitutions by Pd, Ir and Au. The depression of T_c with impurity content and the increase in the residual resistance, ρ_0 , are summarised in figure 5 and 6. Whereas the effects of Y and Th substitutions are rather linear on T_c and quite similar for the different substitutions at the uranium site, we find large discrepancies for substitutions at the platinum site with strongly non-linear behaviour in all cases. The initial concentration dependence of T_c is much steeper for Ir and Au substitutions compared to Pd. Specific-heat results for Pd, Y and Th substitutions are shown in figs 5 and 6 of reference 7. The same type of data for the Ir and Au substitutions are presented in figs 7 and 8 of this paper. Most

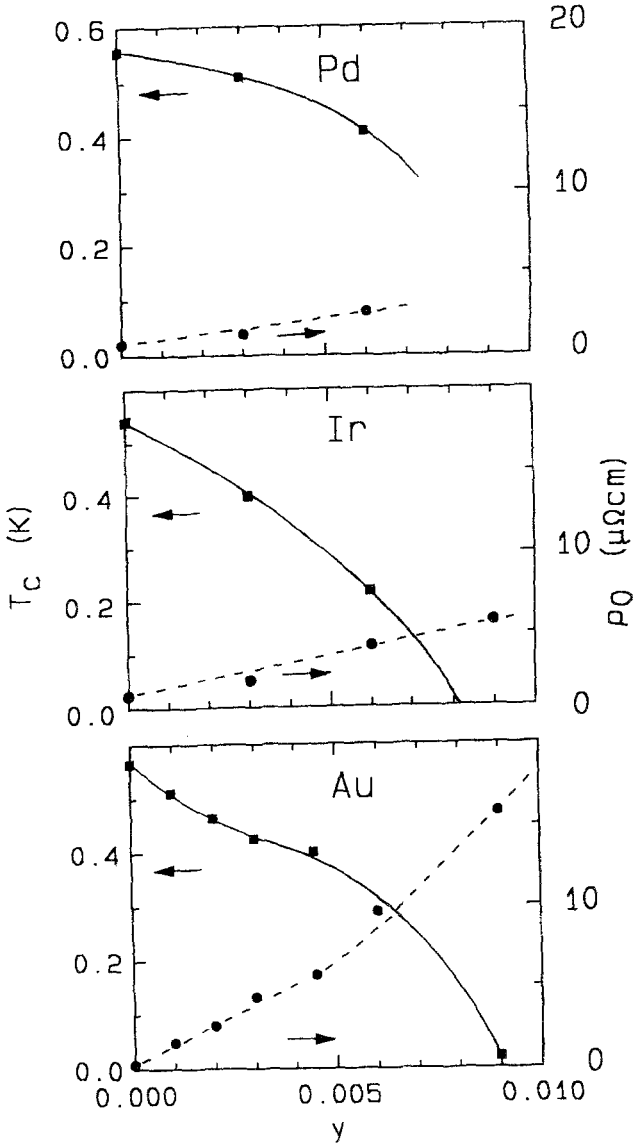


Fig. 5. The superconducting transition temperature, T_c , and the residual resistance, ρ_0 , of $UPt_{3-y}B_y$ plotted as a function of y for different substitutions at the Pt sites; solid lines are guides to the eye.

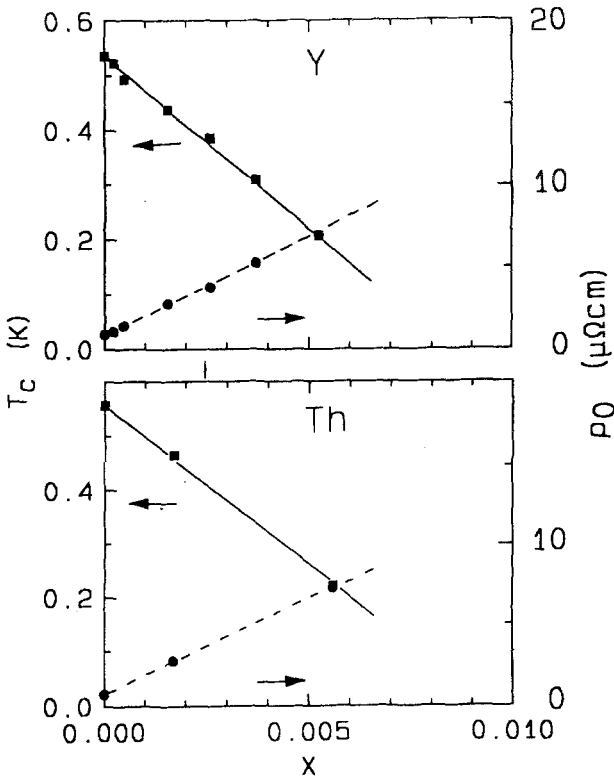


Fig. 6. The superconducting transition temperature, T_c , and the residual resistance, ρ_0 , of $U_{1-x}A_xPt_3$ plotted as a function of x for different substitutions at the U sites; solid lines are guides to the eye; data from ref.19.

remarkable in these results is the apparent enhanced splitting of the double superconducting transition for Pd substitutions, an enhancement that is absent for the other substitutions. For the Y and Pd substitutions, these results have recently been analysed by Vorenkamp *et al.*⁷ For both impurities Δc , the jump in the specific heat at the transition to superconductivity, is depressed at a higher rate than T_c , the superconducting transition temperature, pointing to pair-breaking effects in the depression of the superconductivity. A similar analysis for the other substitutions is still waiting. As already mentioned, the distance in temperature between the two superconducting transitions increases with increasing Pd content. These results might point to a coupling between the superconducting and magnetic order parameters, provided that the weak antiferromagnetic moment increases with Pd concentration. A hint to uranium-moment formation in Pd-substituted UPt_3 comes from the observed long-range antiferromagnetic order in the 5% substituted alloy.

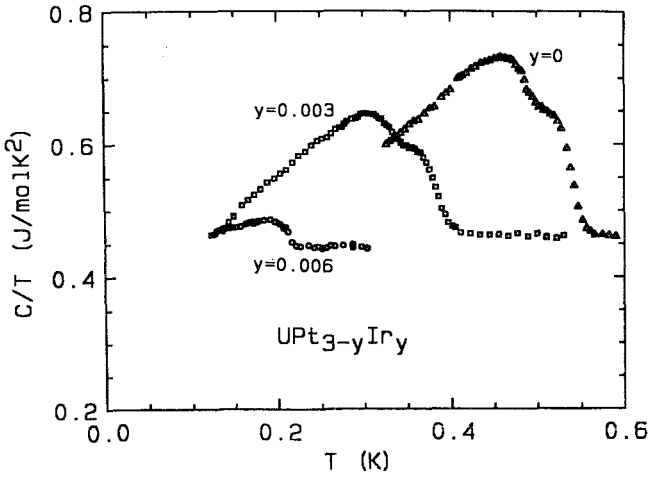


Fig. 7. Specific heat, plotted as c/T versus T , for three annealed polycrystalline samples of $UPt_{3-y}Ir_y$; data from ref.19.

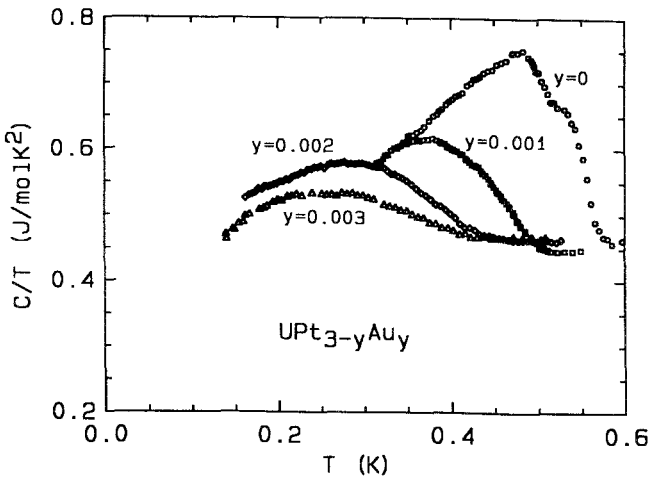


Fig. 8. Specific heat, plotted as c/T versus T , for three annealed polycrystalline samples of $UPt_{3-y}Au_y$; data from ref.19.

However, the same magnetic ordering phenomena occur in the Th-²¹ and Au-²² substituted alloys without comparable effects on the splitting between the two superconducting transitions. Microscopic information on the magnetic properties of the dilute alloys is indispensable before reaching further conclusions.

4. GINZBURG-LANDAU DESCRIPTION FOR THE MULTI-COMPONENT PHASE DIAGRAM IN UPT₃

In the Ginzburg-Landau approach, the double superconducting transition can be attributed to the lifting of the degeneracy of a vector order parameter $\eta = (\eta_1, \eta_2)$ by a symmetry-breaking field. The free energy for a hexagonal system in a two-dimensional representation with a symmetry-breaking field is given by ⁹⁻¹¹:

$$F = \alpha |\eta|^2 + \frac{1}{2}\beta_1 |\eta|^4 + \frac{1}{2}\beta_2 |\eta^2|^2 - \delta\{|\eta_1|^2 - |\eta_2|^2\}$$

with $\alpha = \alpha(T - T_{co})$ and $\delta \propto |\mu|^2$ in case the weak antiferromagnetic order is supposed to be the symmetry-breaking field.

For $\mu \neq 0$, the superconducting transition is split into two transitions at T_{c1} and T_{c2} with specific heat jumps $\Delta c(T_{c1})$ and $\Delta c(T_{c2})$, respectively.

The following expressions can be derived (Joynt,⁹ Machida *et al.*,¹⁰ Hess *et al.*¹¹):

$$T_{c1} = T_{co} + \delta/\alpha_o \quad \Delta c(T_{c1}) = T_{c1}\alpha_o^2/(\beta_1 + \beta_2)$$

$$T_{c2} = T_{co} + \delta\beta_1/\alpha_o\beta_2 \quad \Delta c(T_{c2}) = T_{c2}\alpha_o^2/\beta_1$$

The predicted phase diagram for UPt₃ in the (B,T) plane, is different for B parallel and perpendicular to the hexagonal axis. The suppression of the splitting of the superconducting transition that is observed for uniaxial pressures along the c-axis above 2-3 kbar¹⁶ can be explained by a vanishing of the symmetry-breaking field as neutron experiments show that the weak antiferromagnetic moment vanishes around the same pressure.²³ A double superconducting transition in zero field is compatible with $\beta_2/\beta_1 > \alpha_o T_{co}/\delta > 0$ at non-zero δ -values. In the absence of a symmetry-breaking field ($\delta = 0$), the model predicts the B phase to be stable for $\beta_2/\beta_1 > 0$, whereas a mixed state of the phases A and C is found for the interval $-1 < \beta_2/\beta_1 < 0$. The experimental value for the ratio β_2/β_1 amounts to 0.4 approximately and is found slightly to increase under uniaxial pressure along the c-axis¹⁶ pointing to positive values for β_2/β_1 in the studied pressure interval. Therefore, the B phase is predicted to be the stable phase under uniaxial pressure along the c-axis in this model.

5. THE SUPERCONDUCTING PHASE DIAGRAM STUDIED BY DILATATION

Extensive studies have recently been devoted to the study of the multicomponent superconducting phase diagram of UPt₃ for different field orientations^{8,24} by means of dilatometry studies. As mentioned in the introduction, three different

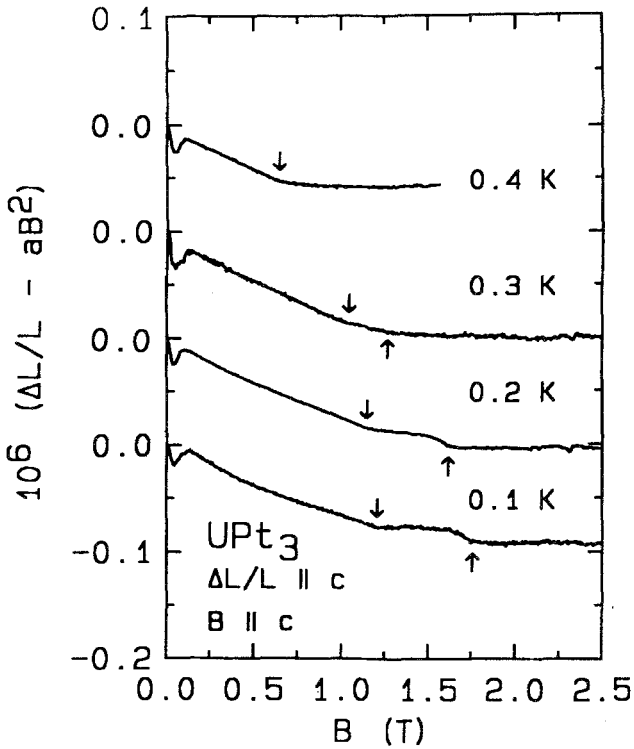


Fig. 9. Magnetostriction along the c-axis for fields applied along the c-axis at different temperatures; the quadratic background of the normal-state magnetostriction has been subtracted; the anomalies at the superconducting transitions are indicated by arrows; the low-field anomaly at $B=0.1$ T is also observed above 0.5 K and persists to exist up to temperatures of a few kelvin; data from ref.24.

phases have been recognised in thermodynamic, transport and acoustic measurements. Additional experiments have been performed under uniaxial and hydrostatic pressures to verify the stability of the different phases against lattice-parameter variations. Impurity studies have already been discussed in the previous section. The thermodynamic stability of the phase diagram, in particular the crossing of four second-order phase lines in a tetracritical point has recently been explored by Van Dijk et al.^{8,24} in thermal-expansion and magnetostriction studies in the temperature range between 80 and 600 mK under applied magnetic fields up to 9 tesla. Experiments have been performed by means of a three-terminal capacitance method on a single-crystalline UPt_3 sample with typical dimensions of a few millimeters with a sensitivity for relative length changes of 10^{-9} . Scans have been made at constant temperature as a function of the applied magnetic field for various combinations of field and measuring directions with respect to the crystallographic axes and as a function of temperature at constant field values. An example of these studies is

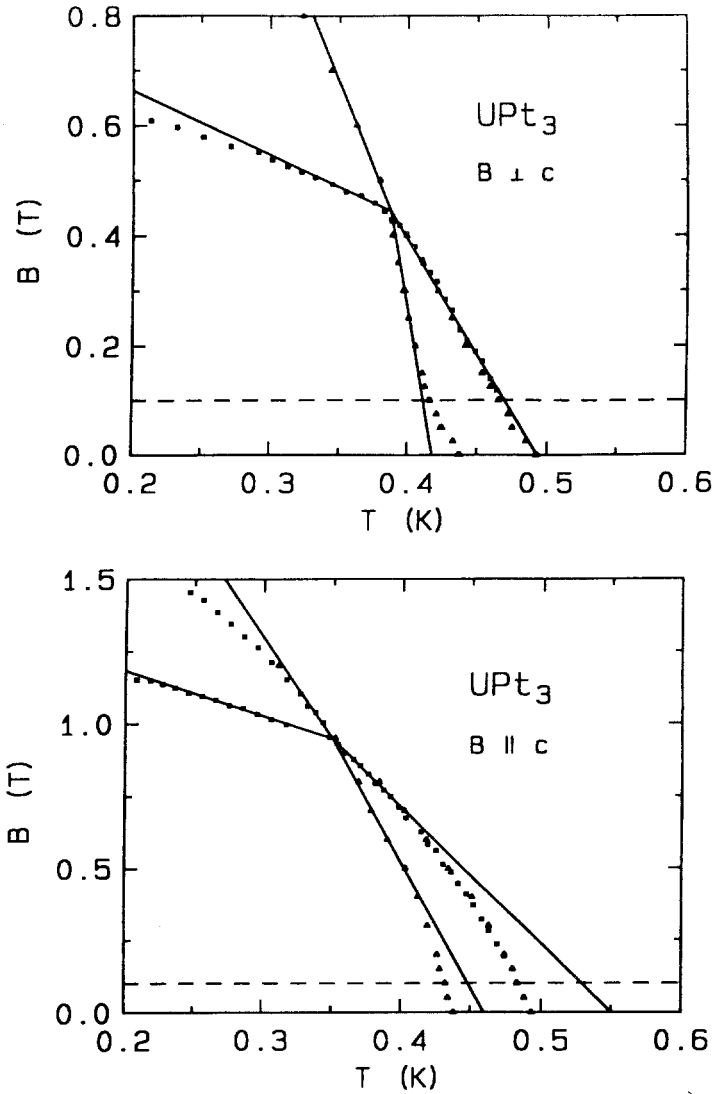


Fig. 10. The superconducting phase diagram of UPt_3 near the tetracritical point for fields perpendicular (a) and parallel (b) to the hexagonal axis; solid lines represent the fitted slopes of the phase lines near the tetracritical point; the dashed line indicates the low-field anomaly at $B=0.1$ T; data from ref.24.

shown in fig. 9, where magnetostriction data are presented. From these experiments the superconducting phase diagrams have been constructed for fields parallel and perpendicular to the hexagonal axis, see fig. 10. For both field directions, the phase diagram shows three superconducting phases which meet at a tetracritical point. It has been demonstrated that the measured phase diagrams are thermodynamically stable and that all four phase lines are of second order.²⁴ Via Ehrenfest relations, the uniaxial pressure derivatives of the various phases have been determined. From extrapolation of these initial pressure derivatives, the most stable phase under uniaxial pressure along the c -axis is found to be the high-field low-temperature C phase, in clear contrast to the model analysis in the previous section where the B phase was predicted to be the stable phase on the basis of the experimental values for the ratio β_2/β_1 .

6. SUMMARY

In UPt_3 , a double superconducting transition is observed in zero-field thermodynamic measurements for the majority of polycrystalline and single-crystalline samples of UPt_3 . In the B - T plane, a complex superconducting phase diagram has been identified with three distinct phases. This feature of a double superconducting transition has been related in subsequent studies to the presence of either a weak magnetic moment on the uranium sites or an incommensurate structural modulation. Studies on non-stoichiometric compounds, in which additional reflections in the X-ray spectrum are observed with hardly any impact on the double transition, put question marks at the second possibility. Moreover, Vorenkamp et al.²⁵ remark that a kink in the $H_{c2}(T)$ and $H_{c1}(T)$ curves has been observed for samples in which the double transition in the specific heat is masked by the broadness of the superconducting transition. Current models that describe this phase diagram are based on the presence of a symmetry-breaking field. The weak antiferromagnetic order in UPt_3 is certainly a candidate for this symmetry-breaking field, although several questions have to be cleared up. The distance in temperature between the two zero-field superconducting transitions increases with increasing concentration of Pd impurities. This observation seems to support the concept of the symmetry-breaking field since at higher Pd concentrations long-range antiferromagnetic order with uranium moments of about $0.5 \mu_B$ is observed. With the assumption of an increase of the weak antiferromagnetic moment with increasing Pd concentration, the increased splitting finds an elegant explanation. It remains, however, to be explained that a similar increase in the distance between the two transitions is absent in Th- and Au-substituted alloys where long-range antiferromagnetic order is observed as well for comparable concentrations of the substituted elements. Finally, the stability of the different phases under applied uniaxial stress along the c -axis creates a problem since it is the C phase instead of the B phase that seems to be the most stable one under pressure.

ACKNOWLEDGEMENTS

This work is supported by the "Stichting FOM" (Foundation for Fundamental Research of Matter) and by the Centre for sample preparation FOM-ALMOS.

REFERENCES

1. R. Fisher, S. Kim, B. Woodfield, N. Philips, L. Taillefer, K. Hasselbach, J. Flouquet, A. Giorgi and J.L Smith, *Phys.Rev.Lett.* **62** (1989) 1411.
2. K. Hasselbach, L. Taillefer and J. Flouquet, *Phys.Rev.Lett.* **63** (1989) 93.
3. T. Vorenkamp, Z. Tarnawski, H.P. van der Meulen, K. Kadowaki, V.J.M. Meulenbroek, A.A. Menovsky and J.J.M. Franse, *Physica B* (1990) 564.
4. K. Hasselbach, A. Lacerda, A. de Visser, K. Behnia, L. Taillefer and J. Flouquet, *J.Low Temp.Phys.* **81** (1990) 299.
5. G. Bruls, D. Weber, B. Wolf, P. Thalmeier, B. Lüthi, A. de Visser and A.A. Menovsky, *Phys.Rev.Lett.* **65** (1990) 2294.
6. S. Adenwalla, S. Lin, Q. Ran, Z. Zhao, J. Ketterson, J. Sauls, L. Taillefer, D. Hinks, M. Levy and B. Sarma, *Phys.Rev.Lett.* **65** (1990) 2289.
7. T. Vorenkamp, M.C. Aronson, Z. Koziol, K. Bakker, J.J.M. Franse and J.L. Smith, *Phys.Rev.B* **48** (1993) 6373.
8. N.H. van Dijk, A. de Visser, J.J.M. Franse, S. Holtmeier, L. Taillefer and J. Flouquet, *Phys.Rev.B* **48** (1993) 1299 and *Physica B* 186-188 (1993) 267.
9. R. Joynt, *Supercond.Sci.Technol.* **1** (1988) 210.
10. K. Machida, M. Ozaki and T. Ohmi, *J.Phys.Soc.Jpn* **58** (1989) 4116.
11. D.W. Hess, T. Tokuyasu and J.A. Sauls, *J.Phys: Condens.Matter* **1** (1989) 8135.
12. G. Aeppli, E. Bucher, C. Broholm, J.K. Kjems, J. Baumann and J. Hufnagl, *Phys.Rev.Lett.* **60** (1988) 615.
13. P.H. Frings, B. Renker and C. Vettier, *J.Magn.Magn.Mat.* **63& 64** (1987) 202.
14. R. Joynt, V.P. Mineev, G.E. Volovik and M.E. Zhitomirsky, *Phys.Rev.B* **42** (1990) 2014.
15. K. Bakker, A. de Visser and J.J.M. Franse, *J.Magn.Magn.Mat.* **108** (1992) 79.
16. D.S. Jin, S.A. Carter, B. Ellman, T.F. Rosenbaum and D.G. Hinks, *Phys.Rev.Lett.* **68** (1992) 1597.
17. M.C. Aronson, R. Clarke, B.G. Demczyk, B.R. Coles, J.L. Smith, A. de Visser, T. Vorenkamp and J.J.M. Franse, *Physica B* **186-188** (1993) 788.
18. P.A. Midgley, S.M. Hayden, L. Taillefer, B. Bogenberger and H. von Lönheysen, *Phys.Rev.Lett.* **70** (1993) 678.
19. K. Bakker, Thesis University of Amsterdam (1993).
20. J.P. Brison et al. Proc. SCES 93, to be published in *Physica B*.
21. A.P. Ramirez, B. Batlogg, E. Bucher, and A.S. Cooper, *Phys.Rev.Lett.* **57** (1986) 1072.
22. K. Kadowaki, J.C.P. Klaasse, and J.J.M. Franse, *J.Magn.Magn.Mat.* **76& 77** (1988) 233.
23. S.M. Hayden, L. Taillefer, C. Vettier and J. Flouquet, *Phys.Rev.B* **46** (1992) 8675.
24. N.H. van Dijk, A. de Visser, J.J.M. Franse and L. Taillefer, *J.Low Temp.Phys.* **93** (1993) 101.
25. T. Vorenkamp, A. de Visser, R. Wester, A.A. Menovsky, J.J.M. Franse and E.A. Knetsch, *Phys. Rev.B* **48** (1993) 6385.